Novel P/Si Based Nanoparticles for Durable Flame Retardant Application on Cotton

Na Li
Donghua University - Songjiang Campus: Donghua University
Panpan Chen
Donghua University - Songjiang Campus: Donghua University
Dongni Liu
Donghua University - Songjiang Campus: Donghua University
Gaowei Kang
Donghua University - Songjiang Campus: Donghua University
Liu Liu
Donghua University - Songjiang Campus: Donghua University
Liyun Xu
Nantong University
Jianyong Yu
Donghua University - Songjiang Campus: Donghua University
Faxue Li
Donghua University
Dequn Wu (dqwu@dhu.edu.cn)
Donghua University - Songjiang Campus: Donghua University https://orcid.org/0000-0002-1118-8729

Research Article

Keywords: Nanoparticles, Synergistic flame retardant, Durable flame retardant cotton fibers, Dip-coating and plasma induced crosslinking

Posted Date: June 23rd, 2021

DOI: https://doi.org/10.21203/rs.3.rs-585202/v1

Version of Record: A version of this preprint was published at Cellulose on January 23rd, 2022. See the published version at https://doi.org/10.1007/s10570-021-04309-4.

Abstract

Cotton fibers as original materials of cotton fabrics have a widely application due to its perfect hygroscopicity, air permeability and largest annual output. However, cotton materials have potential safety hazard during its application because of flammability (limiting oxygen index is about 18%). In order to improve the flame retardancy of cotton fibers and reduce the damage of its mechanical properties, novel P/Si based flame retardant (PFR) nanoparticles were synthesized by one-step radical polymerization. Vinyl phosphoric acid and tetramethyl divinyl disiloxane were introduced into the nanoparticles. The structure, morphology and thermal stability of PFR was characterized by fourier transform infrared spectroscopy (FT-IR), field emission scanning electron microscopy (FE-SEM), thermogravimetric analysis test (TGA). Durable flame retardant cotton fibers were prepared by dip-coating and plasma induced crosslinking methods. Micro-calorimeter (MCC) characterization showed that the peak of heat release rate (pHRR) and the total heat release were reduced by 47.3% and 29.8% for modified cotton fibers compared with pure cotton fibers. Limiting oxygen index (LOI) of modified cotton fibers was increased to 27%. The residue carbon of modified cotton fibers was 19.0% at 700 o C, while the value of pure cotton fibers was 3.0%. Besides, durability of the modified cotton fibers was approved by cyclic washing test. In addition, flame retardant mechanism was revealed by collecting and analyzing condensed and gaseous pyrolysis products. The data of FE-SEM for residue carbon, FT-IR spectra of products at different pyrolysis temperatures and pyrolysis gas chromatography mass spectrometry (Py-GC-MS) showed that PFR was a synergistic flame retardant contained barrier and quenching effecting applied on cotton materials.

Introduction

Textiles have already permeated in every household. Among them, natural fiber products are most favored. Cotton fibers as the original materials of cotton fabrics have a widely application (Zhang et al. 2021) due to their perfect hygroscopicity, air permeability, and a large annual output (Mathangadeera et al. 2020; Schumacher et al. 2020). However, the limiting oxygen index (LOI) of pure cotton materials is about 18%, flammability of cotton fibers makes them as a potential safety hazard material during use (Cheema et al. 2013). Therefore, it has practical significance to improve the flame-retardant properties of cotton marertals.

Nowadays, the methods of endowing function to cotton materials are mainly focused on surface modification, such as coating (Li et al. 2011; Alongi et al. 2013; Pan et al. 2017), layer by layer, grafting and so on (Alongi et al. 2011; Alongi et al. 2014; Indraneel et al. 2017; Li et al. 2019; Wang et al. 2020). Surface modification is an effective and convenient method to offer flame-retardant properties to combustible materials (Kim et al. 2014). Firstly, most flame retardants are concentrated on the surface of the protected textiles to achieve the highest protection. Secondly, flame-retardant layers do not alter the mechanical properties of the protected textiles. Thirdly, flame-retardant layers can be integrated with functional components purposely to achieve multiple functions (Chen et al. 2015). Compared with coating and layer-by-layer self-assembly, grafting method has stronger durability via connecting the flame

retardant with the substrate through chemical bonds. Plasma has been explored widely to graft cotton fabric by inducing crosslinking. Tsafack et al. investigated the simultaneous grafting and polymerization of flame retardant monomers on cotton fabric induced by argon plasma (Tsafack et al. 2008). Edwards et al. prepared two new types of amino phosphate monomers and applied them to cotton by atmospheric pressure plasma treatment (Edwards et al. 2012). Shahidi et al. utilized low temperature plasma technology to endow cotton fabric with anti-UV and flame retardant (Shahidi et al. 2014). Plasma is an effective path to modify surface of cotton material.

Besides, flame retardant as a functional additive to improve the flame retardancy of polymers was attracting more attention. Both industrial and academic researchers have focused their efforts on the design and development of chemicals to prevent the combustion or delay the spread of flame after ignition since the 1960 s (Horrocks et al. 2012). Among the synergistic flame retardant, phosphorus-based compounds represent a suitable alternative to halogen-based flame retardants (Alongi et al. 2013). Hou et al. modified two-dimensional Co-based metal organic framework by conjugating DOPO to prepare organic and inorganic hybrid phosphorus flame retardant (Hou et al. 2018). Pethsangave et al. synthesized a phosphorus functionalized polymer-based graphene composite as an efficient flame retardant (Pethsangave et al. 2019). Effective flame retardancy depends on the interaction between the flame retardant and the matrix strongly, as well as the structure-property relationship between them in process of thermal decomposition. The mode of action can be classified into condensed and gas-phase mechanisms generally and many successful phosphorus flame retardants include both of them (Rabe et al. 2017). Yang et al. established P and N flame retardant to reduce the fire hazard of epoxy resin (et al. (2019). Balabanovich et al. prepared the P and Si system to achieve synergies and enhance flame retardant of polyester (Balabanovich et al. 2009). Sun et al. (2021) synthesized a P/N based flame retardant to reduce the flammability of cotton (Sun et al. 2021). Synergetic flame retardant has become the dominant topic in the field of flame retardant. Eco-friendly and sustainability play guiding roles in novel flame retardant system (FRs) (Velencoso et al. 2018). In order to improve the compatibility between flame retardant and matrix, reduce damage of mechanical properties, the FRs are fabricated into nano scale. Jiang et al. (2018) explored mesoporous silica as the carrier for flame retardant modification to improve the compatibility of epoxy resin (Jiang et al. 2018). Wicklein et al. prepared heat insulation and flame retardant light anisotropic foam based on nanoscale cellulose and graphene oxide (Wicklein et al. 2015).

In this research, novel nanoparticle flame retardant containing phosphorous and silicon elements was synthesized by one-step reaction of free radical polymerizationto achieve synergistic efficiency. Vinyl phosphoric acid (VA) and tetramethyl divinyl disiloxane (THOD) were introduced during synthesis process. Plasma induce crosslinking method was utilized to connect nano flame retardant and cotton fibers to realize the intrinsic flame retardancy. Multiple flame retardant performance indicators were evaluated. In addition, durable flame retardancy was tested and flame retardant mechanism was revealed. Besides, the effect of nanoparticles on the mechanical properties of cotton fibers was also investigated.

Materials And Methods

2.1 Materials and chemicals

3,3,5,5-tetramethyl-3,5-disila-4-oxa-1,6-heptadiene (TDOH) was supplied by Gaip Chemical (Shanghai, China) Co., Ltd. Vinyl phosphoric acid (VA) was supplied by Tokyo Chemical Industry co., ltd. 2, 2'-azobis [2-methylpropionamidine] dihydrochloride (AIBA) was purchased from Aladdin Biochemical Technology (Shanghai, China) Co., Ltd. All of chemicals are analytical grade without further purification before use. Cotton fiber was provided by Yongyue Textile Technology Co., Ltd.

2.2. Synthesis of flame retardant containing P and Si

The flame retardant was synthesized by radical polymerization as shown in scheme 1. Typically, TDOH (11.16 g, 0.06 mol) and VA (12.96 g, 0.12 mol) were dissolved in distilled water (10 mL) and placed in a three-neck flask, using AIBA (0.50 g, 0.0018 mol) as catalyzer. The mixture was heated up to 70 ^{o}C with mechanical stirring for 2 h. Then, the nanoparticles were obtained by centrifugation and freeze-drying, designating as PFR. (yield 83.1%).

2.3 Preparation of flame retardant modified cotton fibers

The preparation of flame retardant cotton fibers involved two steps: dip-coating of PFR precursor and radio frequency capacitively-coupled plasma (RF-CCP) treatment (Malshe et al. 2012). In detail, the PFR (0.40 g) was ultrasonic dispersed in ethanol solution (50 mL). Cotton fibers (2.00 g) were placed in the solution and dipped for 1 h, dried in vacuum oven at 70 ^{o}C. Coated cotton fibers were treated by plasma for 60 s in RF-CCP reactor (AP600, Nordson-March, USA) with 13.56 MHz, the RF power was 50 W and plate distance was 10.16 cm. The reactor was pumped down to a base pressure of 20 mTorr and then the argon gas was introduced into the chamber to reach 200 mTorr for plasma generation. The treated fibers were achieved and designated as pCo-PFR after ultrasonic washing for 15 mins, drying in an oven at 70 ^{o}C. The weight gain rate (A) was calculated by weighting method of Eq. (1). In addition, cotton fibers of plasma treated without dipping in the PFR dispersion were taken as contrast sample, and designated as pCo. Pure cotton fibers were conducted as control sample and named as Co.

$$A = \frac{wf - wi}{wi} \qquad (1)$$

In this equation, W_f is the weight of the modified cotton fibers and W_i is the weight of the pure cotton fibers.

2.4 Measurements

Field Emission Scanning Electron Microscope (FE-SEM) images were obtained with Hitachi SU8010 to observe the morphology of PFR and cotton fibers at ambient temperature. In details, the cotton fibers before and after modification were observed. All the samples were sputter-coated with a conductive gold layer before FE-SEM testing.

Element analysis (EA) and inductive coupled plasma emission spectrometer (ICP) experiments were performed by using an Elmentar Vario EL III-EA and Prodigy-ICP to determine the element composition of nanoparticles. The samples were diluted in deionized water to 20 mL suspension for testing.

Fourier Transform Infrared (FTIR) spectra of PFR was recorded in the 4000-500 cm^{-1} spectral region via a Thermo Fisher Nicolet 6700 under the resolution of 4 cm^{-1}.

Thermal gravimetric analysis (TGA) was performed to evaluate the thermal and thermo-oxidation decomposition of PFR, pure and grafted cotton fibers via German NETZSCHTG209F1 instrument. About 5 mg samples were heated from 30 ^{o}C to 700 ^{o}C under continue nitrogen or air atmosphere with a heating rate of 10 ^{o}C/min.

X-ray photoelectron spectra (XPS) were recorded on Thermo ESCALAB 250XI to test the contents of silicon and phosphorus elements on the surfaces of modified cotton fibers.

Limiting oxygen index (LOI) was tested by Qingdao zr-1 according to the testing method for flame retardant property of viscose staple fibers-oxygen index (FZ/T 50016-2011). The cotton fibers (20 g) were spun (linear density ≤ 60 tex) into yarn. The cotton yarn (0.9 g) was knotted and twisted in 120 twists, and folded in half to form a strand as test spline. The dimensions of specimen were 75 mm. The samples were pre-humidified according to GB/T 6529 standard. Five specimens were tested for each composition.

The microscale combustion calorimeter (MCC) (Fire Testing Technology Ltd., UK) was employed to evaluate the combustion behavior. The sample (5 mg) was heated from room temperature to 700 °C at a heating rate of 1 °C/s according to ASTM D7309-2007. Three specimens were tested for each composition.

Durable determination of modified fibers was tested according to procedure 5 N of standard ISO 6330: 2012, MOD, hang to dry mode (Han et al. 2019).

Pyrolysis Gas Chromatography mass spectrometry (Py-GC-MS) test was conducted to analysis modified cotton fiber pyrolysis behaviors and products by using GCMS-QP 2010 from Shimadzu Corporation of Japan and a Frontier single-point cracker in Japan. The pyrolysis temperature was 380 °C, and the pyrolysis products were separated and identified by a coupled GCMS-QP2010 gas chromatograph mass spectrometer. Mass spectrometry conditions: EI source, mass-to-charge ratio m/z range 30~600, searched using Nist107 mass spectrometry library.

The mechanical properties of the samples were determined by tensile measurements with a YG001B testing machine according to standard method ASTM D5035-2011. The tensile speed was 10 mm/min.

The pretension was 0.2 cN/dtex. The spacing length of the upper and lower grippers was 10 mm. Each sample was tested 50 times.

Results And Discussion

3.1 Formation and morphology of PFR

Radical polymerization reaction was employed as a convenient and simple synthesis method to obtain nanoparticles as shown in scheme 1. The morphology of nanoparticles PFR was obtained by FE-SEM. In Figure 1a, PFR exhibited nano agglomeration and the particle size was about 25~30 nm. The element and content were determined by element analysis (EA) and inductive coupled plasma emission spectrometer (ICP) as shown in Table 1. The chemical structures of PFR were estimated via FTIR (Fig. 1b). In the FTIR spectrum of PFR, the symmetric stretching vibration peaks of =C-H at about 3051 cm^{-1} and 2963 cm^{-1} disappeared. The symmetric stretching vibration peaks at about 1593 cm^{-1} and 1610 cm^{-1} attributed to C=C also disappeared. Besides, the stretching vibration peak of Si-C or P-C appeared at 840~670 cm^{-1} (Zope et al. 2017). The stretching vibration peak of Si-O appeared in the wavenumber range of 1090~920 cm^{-1} (Guo et al. 2020; Jian et al. 2020). The data indicated the successful synthesis of PFR.

Table 1 The element analysis of PFR

Element	C	H	O	Si	P
Content percentage (%)	42.32	8.75	24.56	7.31	16.15

3.2 Thermal stability of PFR

The thermal stability of PFR was analyzed by thermogravimetric analysis (TGA) under continuous nitrogen and air atmosphere from 30 ^{o}C to 700 ^{o}C. The results (Figure 1c and d) showed that the residue weight percent (CR) of PFR was 70.2% at 700 ^{o}C in nitrogen, while the CR was 30.1% in atmosphere environment. In air, PFR showed two-phase thermal degradation. The maximum decomposing rate (T_{max}) occurred at about 480 ℃ in nitrogen and 240 ^{o}C. This might be due to the conversion was easier of phosphorus into phosphate and phosphonate compounds was easier in aerobic environment (Lazar et al. 2020). All the data certificated PFR had high thermal stability.

3.3 Morphology and structure of flame retardant modified cotton fibers

Cotton fibers as the original material of cotton fabric were modified with the PFR to reduce flammable property by dip-coating and radio frequency capacitively-coupled plasma (RF-CCP) treatment as shown in graphic abstract. Seen from the images of FE-SEM (Fig. 2), it could be observed that there were visible grooves and natural spirals on the surface of raw cotton fibers (Co), while plasma without dip-coating treated cotton fibers (pCo) presented obvious grooves and scratches compared with Co. The dip-coating

and plasma induced crosslinking cotton fibers (pCo-PFR) apperanced attached particles on the surface compared with Co and pCo.

In order to further confirm the crosslinking reaction of PFR and cotton fibers, the FT-IR and XPS of Co and modified cotton fibers were tested. As shown in Fig. 3a, compared with the FT-IR spectrum of Co and pCo, the FT-IR spectrum of pCo-PFR exhibited obvious new absorption peak at about 1260 cm^{-1} and 799 cm^{-1}, which mainly due to the stretching vibration peak of P=O and Si-C (Zope et al. 2017; Guo et al. 2020). There was no significant difference between the FT-IR spectrum of Co and pCo, except for the peak area of hydroxyl group was reduced in FT-IR spectrum of pCo. The above results indicated that one-step of plasma induced crosslinking had no obvious effect on the fiber structure or elements. New structure and element units appeared on the fiber surface after the process of dip-coating and plasma induced crosslinking. In addition, the XPS spectra corresponded to the conclusion of the FT-IR. In Fig. 3b, compared with XPS spectra of Co, the new binding energy was found on spectrum of pCo-PFR at 150.5 eV, 130.6 eV and 99.8 eV, which could be assigned to Si2s, P2p and Si2p, respectively (Chu et al. 2018). The C_{1s} XPS spectra of Co and pCo-PFR were shown in Fig. 3c. The new peak appeared was distinguished as Me_2CO (287.6 eV) on C_{1s} XPS spectra of pCo-PFR, certificated the new structure was formed.

3.4 Thermal stability of nano flame retardant modified cotton fibers

The thermal stability of nanoparticles modified cotton fibers were assessed by thermogravimetric analysis (TGA) under continuous nitrogen from 30 ^oC to 700 ^oC. The heating rate was 10 ^oC/min. As shown in Fig. 4 and Table 2, the residue weight percent (CR) of pCo-PFR was 19.0 % at 700 ^oC. At the same test condition, the CR of Co and pCo were 3.0% and 3.2%, respectively. The CR of pCo-PFR was higher than the Co and pCo distinctly, and also higher than theoretical CR of pCo-PFR. The results confirmed that PFR not only made cotton fibers develop higher residual carbon, but also promoted the fibers to form carbon by themselves. Mass loss rate @ T_{max} of pCo-PFR decreases from -34.6 %/^oC to -28.7 %/^oC, indicated that addition of PFR slowed down the degradation of cotton fibers. In terms of initial degradation temperature ($T_{5\%}$) and fastest degradation temperature (T_{max}), pCo-PFR was more sensitive than Co. This phenomenon was explained by the decomposition of phosphorus to catalysis the formation of carbon in the fibers at lower temperature (Li et al. 2021).

Table 2. Thermogravimetric Data for the nano flame retardant modified cotton fibers

sample	$T_{5\%}$ (^oC)	T_{Max} (^oC)	Mass Loss rate @ T_{max} (%/^oC)	CR at 700 ^oC (%)	Theoretical CR (%)
Co	230.4	376.2	-34.9	3.0	3.0
pCo	135.2	394.5	-34.6	3.2	3.2
pCo-PFR	213.3	360.6	-28.7	19.0	17.8

3.5 Evaluation durable flame retardancy of nanoparticles modified cotton fibers

Micro calorimeter test has been recognized as one of the most acceptable fire testing apparatus for fiber materials that provides the heat release parameters information to evaluate the fire hazard (He et al. 2018). Fig. 5a and b showed the heat release rate (HRR) curves and total heat release (THR) curves of Co, pCo and pCo-PFR. The peak of heat release rate (pHRR) and THR are significant parameters for evaluating the effectiveness of flame retardant (Wu et al. 2018). It could be observed clearly that pHRR of Co was 451 W/g and the THR was 12.1 kJ/g. Compared with Co, the pHRR and THR values of pCo-PFR were decreased by 47.3 % and 29.8 %, respectively. Compared with pCo, the pHRR and THR values of pCo-PFR were reduced by 37.4 % and 28.0 %, respectively. Furthermore, time to reach peak of heat release rate (t_{pHRR}) is also an important parameter for fire risk assessment, and longer t_{pHRR} means more time for escaping. The data in Table 3 showed t_{pHRR} of Co, pCo and pCo-PFR were 35 s, 34 s and 33 s, respectively. The t_{pHRR} of pCo-PFR was shortened slightly. In order to evaluate the flame retardancy of pCo-PFR contained ignition time (TTI), pHRR and t_{pHRR} comprehensively, the fire performance index (FPI) and fire growth index (FGI) were introduced as following equation (Hong et al. 2013):

$$FPI = \frac{TTI}{pHRR} \quad (2)$$

$$FGI = \frac{pHRR}{t_{pHRR}} \quad (3)$$

Generally, higher FPI value and lower FGI value present a lower fire risk (Wang et al. 2018). In Table 3, FPI of Co, pCo and pCo-PFR were 0.011, 0.015 and 0.042, respectively. FGI of Co, pCo and pCo-PFR were 12.9, 11.2 and 7.2, respectively. All above data proved pCo-PFR had better property of fire suppression and providing more time to escape from the scene of fire. The flame retardant property of pCo-PFR was attributed to the destruction of cyclic combustion through synergistic effects of PFR. In addition, the results of LOI were given in Table 3. Co and pCo were easy to ignite and LOI value were about 18%, while LOI of pCo-PFR increased to 27%. The data revealed that the ignition and combustion abilities both decreased with introduction of phosphorus and silicon contents in the cotton fibers.

Table 3. Micro Calorimeter data and limit oxygen index (LOI) of Co, pCo and pCo-PFR

Sample	TTI (s)	pHRR (w/g)	THR (kJ/g)	t_{PHRR} (s)	FPI	FGI	LOI (%)
Co	5	451	12.1	35	0.011	12.9	18
pCo	6	380	11.8	34	0.015	11.2	18
pCo-PFR	10	238	8.5	33	0.042	7.2	27

The flame retardant durability of dip-coating and plasma induced crosslinking cotton fibers was investigated by physics washing (cycle time was set as 5, 10, 30 and 50) according to ISO 6330: 2012,

MOD standard. As shown in Fig. 5c and Table 4, after 50 washing cycles, the pHRR and THR of pCo-PFR were 399 W/g and 10.3 kJ/g, still decreased by 11.6 % and 14.9 % compared with Co. The data proved dip-coating and plasma induced crosslinking brought stability and durability to flame retardant modified cotton fibers.

Table 4. Durability test of pCo-PFR about heat release rate (pHRR) and total heat release (THR)

Washing circle (times)	0	5	10	30	50
pHRR (W/g)	246	251	292	354	399
THR (kJ/g)	8.5	8.7	9.2	9.9	10.3

3.6 Mechanism analyze of flame retardant modified cotton fibers

To investigate the flame retardancy mechanism in gas phase and/or condensed phase, the microstructures of the residual char were collected after combustion test and analyzed by SEM and FT-IR as shown in Fig. 6 and 7. In Fig. 6, Co presented loose and shapeless structure after combustion, which was attributed to diffuse oxygen and flammable gas forming cyclic combustion. The residue sample of pCo showed loose and chaos state. Differenced from the Co and pCo, carbon residue of pCo-PFR appeared relatively complete and kept the spiral shape of cotton fiber.

The condensed phase products at different decomposition temperatures were analyzed by FT-IR spectroscopy as shown in Fig. 7. The temperature of 330 ^{o}C, 380 ^{o}C, 430 ^{o}C and 600 ^{o}C were important decomposition period for cotton matrix in the TGA test. There was no obvious change in chemical structure whether for Co, pCo or pCo-PFR at 330 ^{o}C. Further degradation at 380 ^{o}C, the dehydrogenation of Co, pCo and pCo-PFR occurred and produced substances of aldehydes, ketones (Pastorova et al. 1993). In the FT-IR spectrum at 430 ^{o}C, the unsaturation of molecular chain in the residue carbon increased, and the conjugation of C = C and C = O made the corresponding infrared absorption peak blue shift (Zhang et al. 2021). At 600 ^{o}C, the degradation was completed basically. The carbon residue with higher C/H ratio could be obtained by deoxidation and dehydrogenation. The stretching vibration peak of Si-C (799 cm^{-1}) was prominent in FT-IR spectrum of pCo-PFR (Li et al. 2019). The results showed that the structure of Si-C migrated to the surface of matrix and carried out condensed phase flame retardant to cut off the heat and oxygen necessary for circulating combustion with the increase of temperature (Nechyporchuk et al. 2017).

Besides, the gas phase pyrolysis of Co and pCo-PFR at 380 ^{o}C were monitored by pyrolysis gas chromatography mass spectrometry (Py-GC/MS) as shown in Fig. 8a. It was reported that decomposition of activated cotton materials was mainly through two competitive pathways (Cai et al. 2018; Qu et al. 2011). Dehydrating and charring produced a coke and a small molecule gas, meanwhile depolymerizing formed non-volatile $_{L}$-glucose liquid, which was a crucial middle product of cotton during the pyrolysis process. $_{L}$-glucose continuous decomposition tended to form small molecule gases and secondary coke, glycolaldehyde, tar, etc. (Zhu et al. 2016). Thus, reducing production of $_{L}$-glucose meant a decrease in

combustible substances. During decomposition of Co, the peak of $_L$-glucose appeared at about 15 min. In contrast, the relative peak area of $_L$-glucose in pCo-PFR's Py-GC/MS spectra reduced by 29.4%. In addition, the peak area percentage of flammable gases produced also decreased by pCo-PFR as shown in Fig. 8, such as furans ((1) and (2)), alcohols ((2) and (3)), ketones (4) and aldehydes (5). The nonflammable small molecules contained phosphorus and silicon elements (6) were produced from the cracking process of pCo-PFR.

So, P and Si elements endowed nanoparticles flame-retardant function through two aspects. In condensed phase, the PFR mediated the formation of char by inducing cyclization, crosslinking, and aromatization/graphitization by dehydration of the polymeric structure. The formation of carbonaceous char reduces the release of volatiles (Camino et al. 2001; Schartel et al. 2016;). In the gas phase, the PFR slow down heat transfer via radical generators and non-flammable gases (Bourbigot et al. 2004; Lazar et al. 2020).

3.7 Mechanical properties

The Mechanical properties of Co, pCo and pCo-PFR were shown in Fig. 9a, b and Table 5. It was found that the breaking strength of Co, pCo and pCo-PFR were 4.22 cN, 3.93 cN and 3.79 cN, respectively. The breaking strength of pCo-PFR was decreased by 10.2 % than that of Co. Linear density of pCo-PFR was slightly higher than that of Co. Considering the fiber fineness, the fracture strength of single fiber of Co, pCo and pCo-PFR were 2.78, 2.49 and 2.26 cN/dtex. Besides, elongation at break of pCo-PFR reduced 8.4 % compared with Co. The mechanical property test showed that the dip-coating and plasma induce crosslinking modification had limited damage of mechanical property to cotton fibers.

Table 5. Mechanical properties of Co, pCo and pCo-PFR

Sample	Breaking strength (cN/dtex)	Elongation at break (%)	Linear density (dtex)
Co	2.77	7.25	1.52
pCo	2.49	6.51	1.58
pCo-PFR	2.26	6.64	1.68

Conclusion

A novel nanoparticle flame retardant was synthesized by radical polymerization of THOD and VA in deionized water. Flame retardant activity assessment demonstrated that the nanoparticle had excellent flame retardant for matrix by synergistic mechanism. For the dip-coating and plasma reduced crosslinking cotton fibers, the pHRR and THR decreased by 47.3 % and 29.8 %, respectively. The durability of the modified cotton fibers was approved by cyclic washing test. The pHRR and THR of pCo-PFR were still reduced at 399 w/g and 10.3 kJ/g after 50 times of washing. Besides, nanoparticle eliminated the influence on mechanical and comfort properties of cotton, reduced the modification dosage and saved

cost. To conclude, flame retardant property enriched application filed of cotton materials based on the nanoparticle.

Declarations

Acknowledgments

The research is supported by the National Key Research and Development Program of China (Project Number 2017YFB0309001), the Natural Science Foundation of Shanghai (18ZR1400400, 18ZR1400500, 20ZR1402100), and the Fundamental Research Funds for the Central Universities and Graduate Student Innovation Fund of Donghua University (CUSF-DHD-2019049).

Conflict of interest

The authors declare that they have no conflict of interest. This article does not contain any studies with human participants or animals performed by any of the authors. Informed consent has been obtained from all individual participants included in the study.

References

1. A.N. Zhang et al. (2021) Construction of durable eco-friendly biomass-based flame-retardant coating for cotton fabrics. Chem. Eng. J. 410: 128361
2. R.W. Mathangadeera et al. (2020) Importance of cotton fiber elongation in fiber processing. Ind. Crop. Prod. 147: 112217
3. D.Q. Schumacher et al. (2020) Industrial hemp fiber: A sustainable and economical alternative to cotton. J. Clean. Prod. 268: 122180
4. H.A. Cheema et al. (2013) Conferring flame retardancy on cotton using novel halogen-free flame retardant bifunctional monomers: synthesis, characterizations and applications. Carbohydr. Polym. 92: 885-893
5. Y.C. Li et al. (2011) Intumescent All-Polymer Multilayer Nanocoating Capable of Extinguishing Flame on Fabric. Adv. Mater. 23: 3926-3931
6. J. Alongi et al. (2013) DNA: a novel, green, natural flame retardant and suppressant for cotton, J. Mater. Chem. A 1: 4779-4785
7. Y. Pan et al. (2017) Influences of metal ions crosslinked alginate based coatings on thermal stability and fire resistance of cotton fabrics. Carbohydr. Polym. 170: 133-139
8. J. Alongi et al. (2011) Novel flame retardant finishing systems for cotton fabrics based on phosphorus-containing compounds and silica derived from sol-gel processes. Carbohydr. Polym. 85: 599-608
9. J. Alongi et al. (2014) Caseins and hydrophobins as novel green flame retardants for cotton fabrics. Polym. Degrad. Stab. 99: 111-117

10. S.Z. Indraneel et al. (2017) Development and evaluation of a water-based flame retardant spray coating for cotton fabrics. ACS Appl. Mater. Interf. 9: 40782-40791
11. P. Li et al. (2019) Ecofriendly flame retardant cotton fabrics: preparation, flame retardancy, thermal degradation properties, and mechanism. ACS Sustain. Chem. Eng. 7: 19246-19256
12. S.H. Wang et al. (2020) Surface coated rigid polyurethane foam with durable flame retardancy and improved mechanical property. Chem. Eng. J. 385: 123755
13. M.J. Kim et al. (2014) Graphene Phosphonic Acid as an Efficient Flame Retardant. ACS Nano 8: 2820-2825
14. S.S. Chen et al. (2015) Intumescent flame-retardant and self-Healing superhydrophobic coatings on cotton fabric. ACS Nano. 9: 4070-4076
15. M.J. Tsafack et al. (2008) Flame retardancy of cotton textiles by plasma-induced graft-polymerization (PIGP). Surf. Coat. Tech. 201: 2599-2610
16. B. Edwards et al. (2012) Towards flame retardant cotton fabrics by atmospheric pressure plasma-induced graft polymerization: Synthesis and application of novel phosphoramidate monomers. Surf. Coat. Tech. 209: 73-79
17. S.L. Shahidi (2014) Novel method for ultraviolet protection and flame retardancy of cotton fabrics by low-temperature plasma. Cellulose 21: 757-768
18. A.R. Horrocks et al. (2012) Zinc stannate interactions with flame retardants in polyamides; part 2: potential synergies with non-halogen-containing flame retardants in polyamide 6 (PA6). Polym. Degrad. Stab. 97: 645-652
19. Y.B. Hou et al. (2018) DOPO-Modified twodimensional Co-based metal-organic framework: preparation and application for enhancing fire safety of poly (lactic acid). ACS Appl. Mater. Interf. 10: 8274-8286
20. D.A. Pethsangave et al. (2019) Novel approach toward the synthesis of a phosphorus-functionalized polymer-based graphene composite as an efficient flame retardant, ACS Sustain. Chem. Eng. 7: 11745-11753
21. S. Rabe et al. (2017) Exploring the modes of action of phosphorusbased flame retardants in polymeric systems, Materials 10: 455
22. G. Yang et al. (2019) Synthesis of a novel phosphazene-based flame retardant with active amine groups and its application in reducing the fire hazard of Epoxy Resin. Hazard. Mater. 366: 78-87
23. A.I. Balabanovich et al. (2009) Pyrolysis study of a phosphorus-containing aliphatic–aromatic polyester and its nanocomposites with layered silicates. Polym. Degrad. Stab. 94: 355-364
24. L. Sun et al. (2021) A novel P/N-based flame retardant synthesized by one-step method toward cotton materials and its flame-retardant mechanism. Cellulose 28: 3249-3264
25. M.M. Velencoso et al. (2018) Molecular Firefighting-How modern phosphorus chemistry can help solve the challenge of flame retardancy. Angew. Chem. Int. Ed. Engl. 57: 10450-10467

26. S.D. Jiang et al. (2018) Biobased polyelectrolyte multilayer-coated hollow mesoporous silica as a green flame retardant for epoxy resin. J. Hazard. Mater. 342: 689-697
27. B. Wicklein et al. (2015) Thermally insulating and fire-retardant lightweight anisotropic foams based on nanocellulose and graphene oxide. Nat. Nanotechnol. 10: 277-283
28. P. Malshe et al. (2012) Functional military textile: Plasma-induced graft polymerization of dadmac for antimic robial treatment on nylon-cotton blend fabric. Plasma Chem. Plasma P. 32833-843
29. H. Han et al. (2019) Inherent guanidine nanogels with durable antibacterial and bacterially antiadhesive properties, Adv. Funct. Mater. 29: 1806594
30. I.S. Zope et al. (2017) Development and Evaluation of a Water-Based Flame Retardant Spray Coating for Cotton Fabrics. ACS Appl. Mater. Inter. 9: 40782-40791
31. W.W. Guo et al. (2020) Construction of durable flame-retardant and robust superhydrophobic coatings on cotton fabrics for water-oil separation application. Chem. Eng. J. 398: 125661
32. L. Jian et al. (2020) Multifunctional flame retarded and hydrophobic cotton fabrics modified with a cyclic phosphorus/polysiloxane copolymer. Cellulose 27: 3531-3549
33. S.T. Lazar et al. (2020) Flame-retardant surface treatments, Nat. Rev. Mater. 5, 259-275
34. F. Chu et al. (2018) A facile strategy to simultaneously improve the mechanical and fire safety properties of ramie fabric reinforced unsaturated polyester resin composites. Compos. Part A 115: 264-273
35. N. Li et al. (2021) Eco-friendly and intrinsic nanogels for durable flame retardant and antibacterial properties. Chem. Eng. J. 415: 129008
36. C. He et al. (2018) Mechanically resistant and sustainable cellulose-based composite aerogels with excellent flame retardant, sound-absorption, and superantiwetting ability for advanced engineering materials. ACS Sustain. Chem. Eng. 6, 927-936
37. J. Wu et al. (2018) New application for aromatic Schiff base: high efficient flame-retardant and anti-dripping action for polyesters. Chem. Eng. J. 336: 622-632
38. N. Hong et al. (2013) Facile preparation of graphene supported Co_3O_4 and NiO for reducing fire hazards of polyamide 6 composites. Mater. Chem. Phys. 142: 531-538
39. J. Wang et al. (2018) Construction of multifunctional $MoSe_2$ hybrid towards the simultaneous improvements in fire safety and mechanical property of polymer, J. Hazard. Mater. 352: 36-46
40. I. Pastorova et al. (1993) Preservation of d-glucose-oligosaccharides in cellulose chars. Carbohydr. Res. 248: 151-165
41. N. Li et al. (2019) Novel eco-friendly flame retardants based on nitrogen-silicone schiff base and application in cellulose. ACS Sustain. Chem. Eng. 8: 290-301
42. O. Nechyporchuk et al. (2017) Wet Spinning of Flame-Retardant Cellulosic Fibers Supported by Interfacial Complexation of Cellulose Nanofibrils with Silica Nanoparticles. ACS Appl. Mater. Interf. 9: 39069-39077

43. W. Cai et al. (2018) Bio-oil production from fast pyrolysis of rice husk in a commercial-scale plant with a downdraft circulating fluidized bed reactor. Fuel Process. Technol. 171: 308-317
44. H. Qu et al. (2011) Thermal degradation and fire performance of wood treated with various inorganic salts. Fire Mater. 35: 569-576
45. L. Zhu et al. (2016) The interactions among the pyrolysis of biomass components based on the PY-GC/MS. Chem. Ind. Eng. Prog. 35: 3879-3884
46. G. Camino et al. (2001) Intumescent materials. Fire retardant mater. 318-336
47. B. Schartel et al. (2016) Flame retardancy of polymers: the role of specific reactions in the condensed phase, Macromol. Mater. Eng. 301: 9-35
48. S. Bourbigot et al. (2004) Recent advances for intumescent polymers, Macromol. Mater. Eng. 289: 499-511

Scheme 1

Scheme 1 can be found in the Supplementary FIles.

Figures

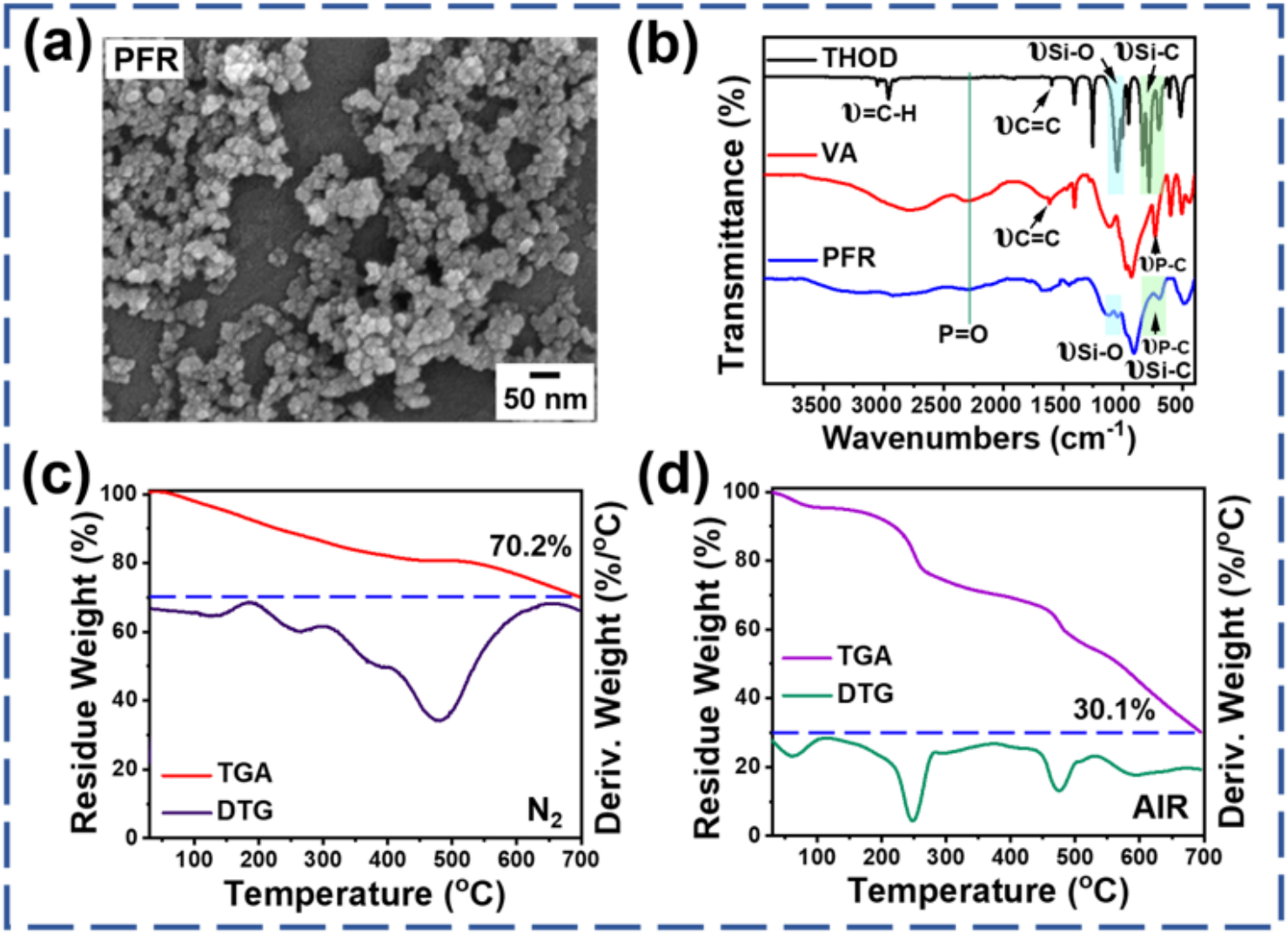

Figure 1

(a) The FE-SEM images of PFR. (b) FT-IR spectra of THOD, VA and PFR. (c), (d) TGA and DTG curves of PFR in nitrogen and atmosphere, respectively.

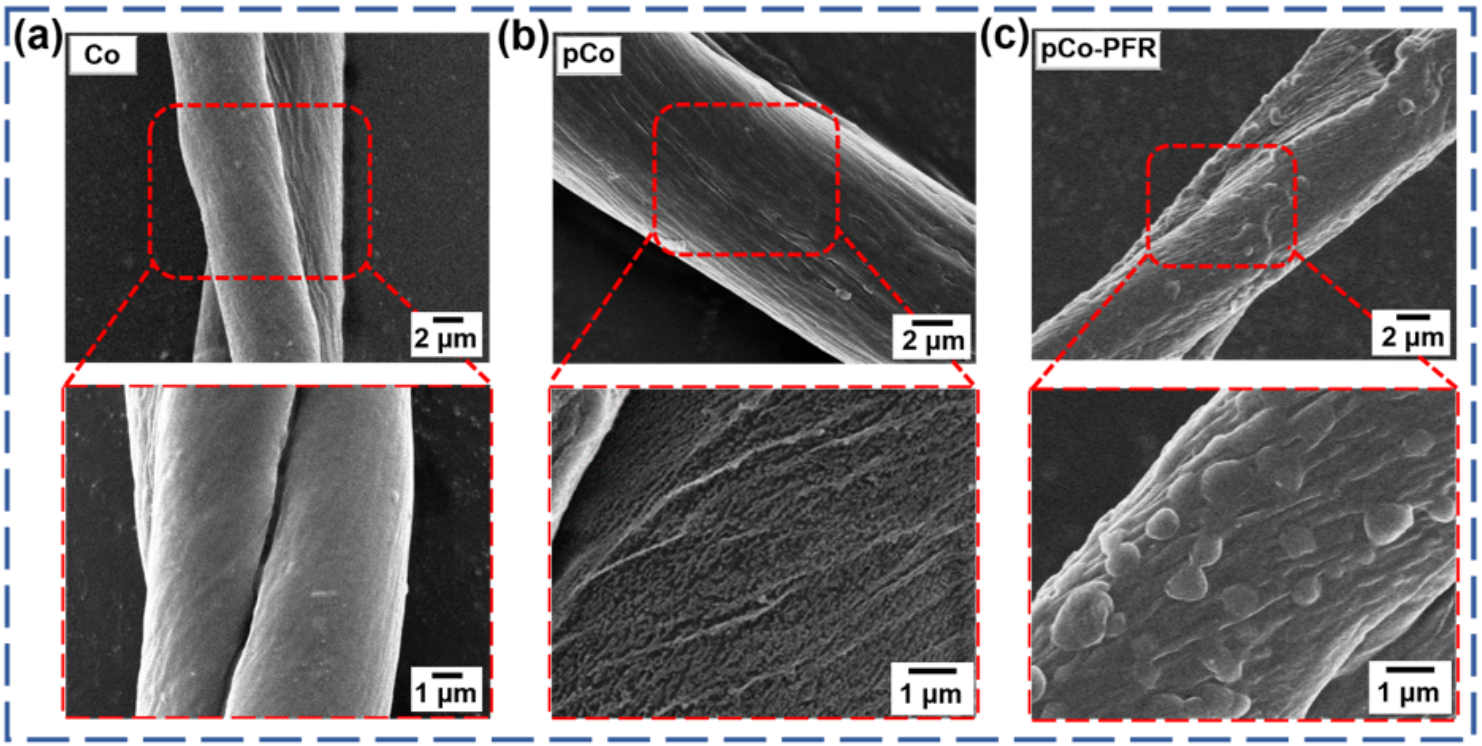

Figure 2

The FE-SEM images with different magnification of Co, pCo and pCo-PFR.

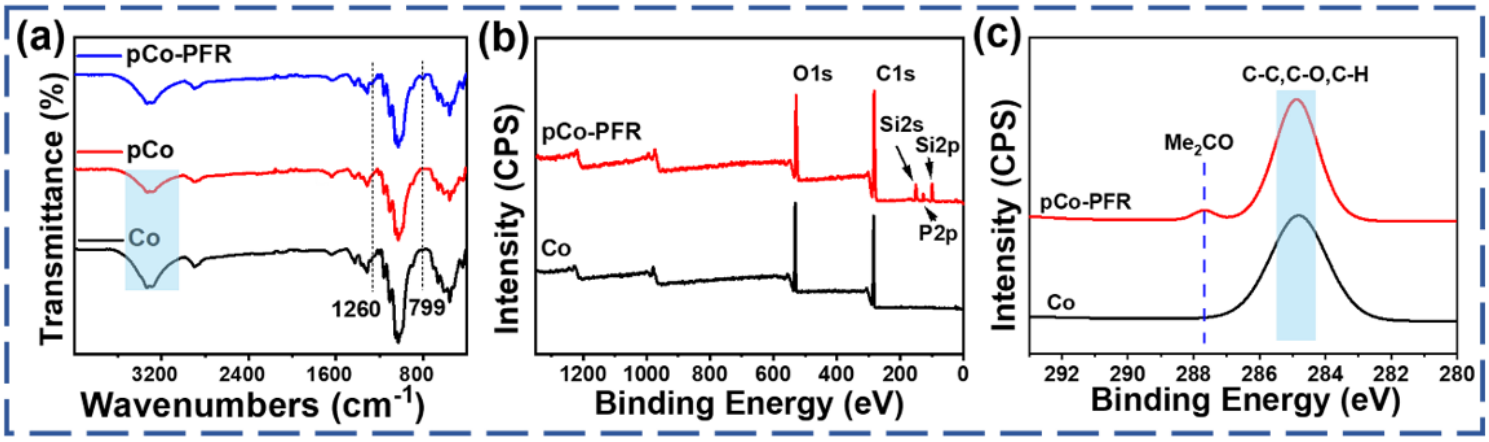

Figure 3

(a) FT-IR spectra and (b) XPS survey of Co and pCo-PFR. (c) C1s XPS spectra of Co and pCo-PFR.

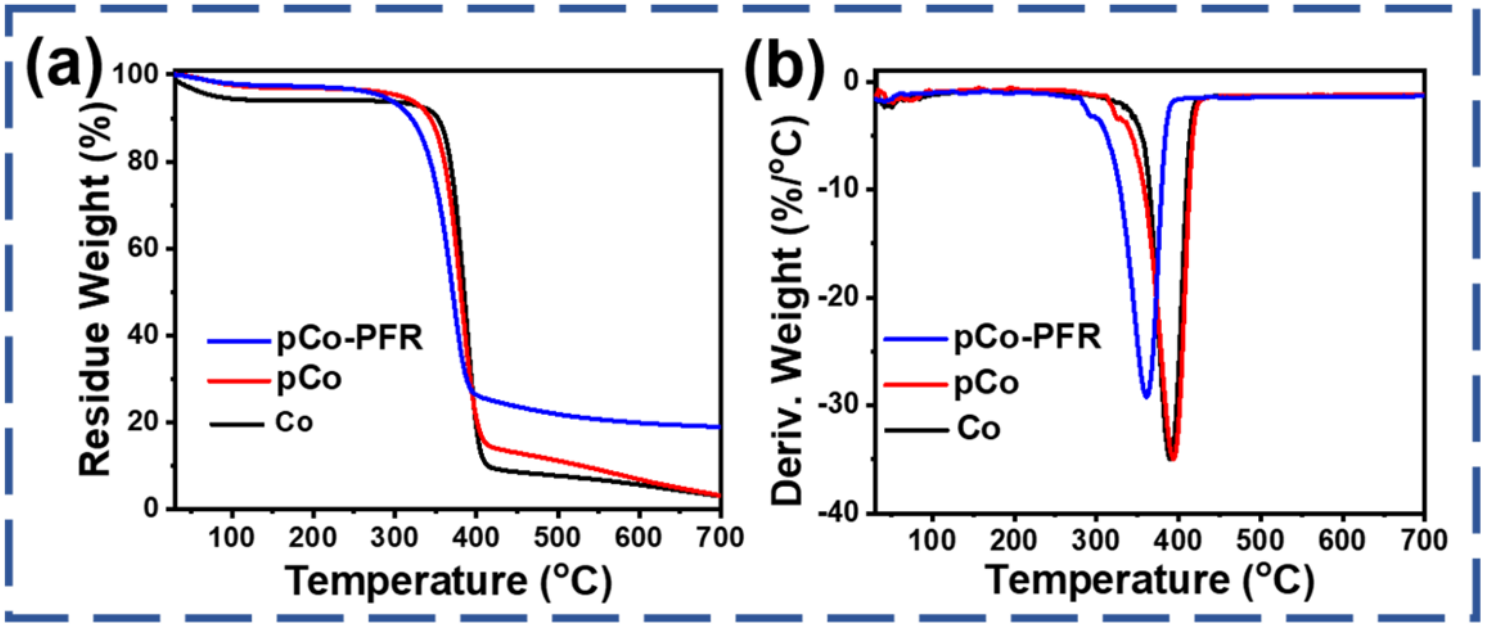

Figure 4

Thermal properties of cotton fibers and modified cotton fibers in nitrogen. (a) The TGA curves. (b) The DTG curves.

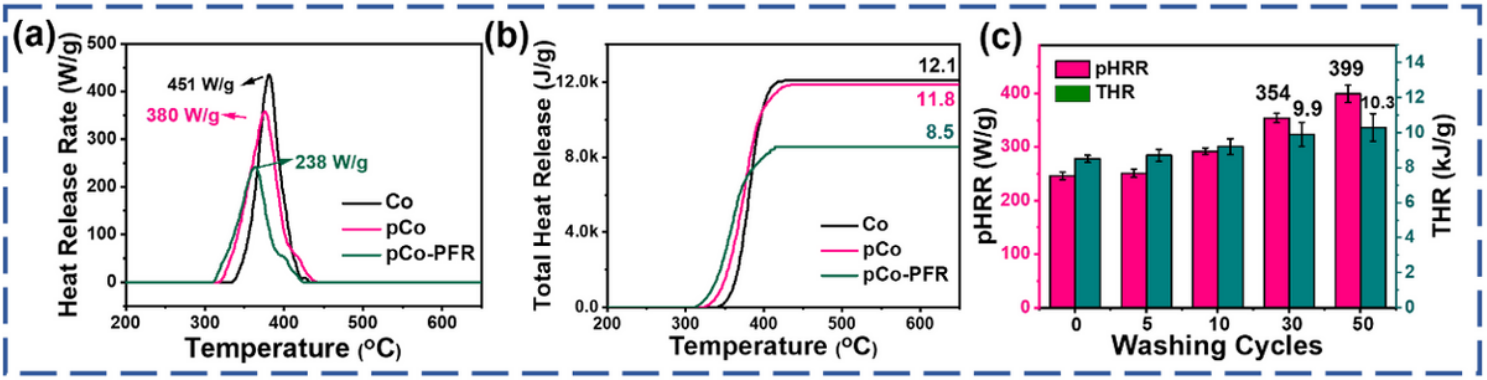

Figure 5

Micro calorimeter test curves of Co, pCo and pCo-PFR. (a) The curves of heat release rate. (b) The curves of total heat release. (c) 50 times cycle washing test of pCo-PFR about heat release rate and total heat release.

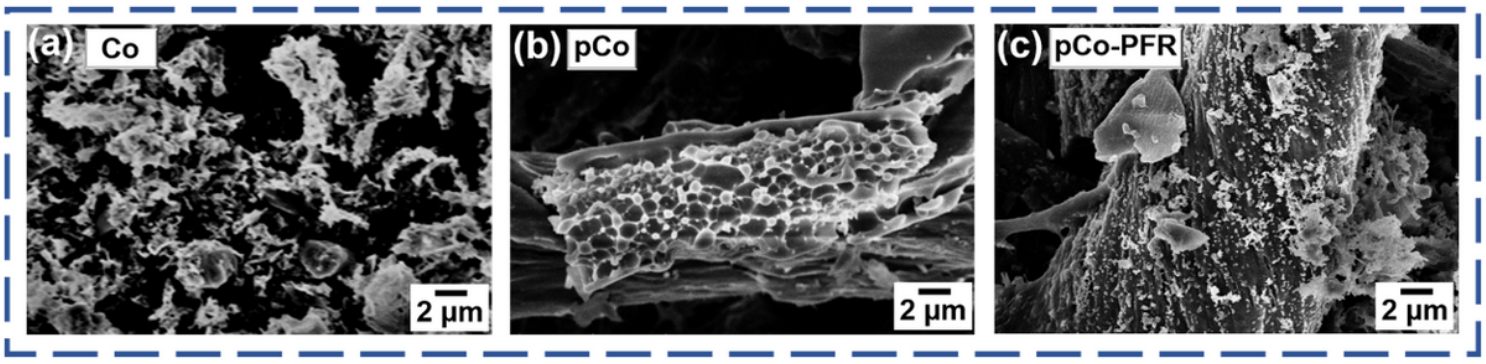

Figure 6

Different magnification SEM images of Co, pCo and pCo-PFR after combustion test.

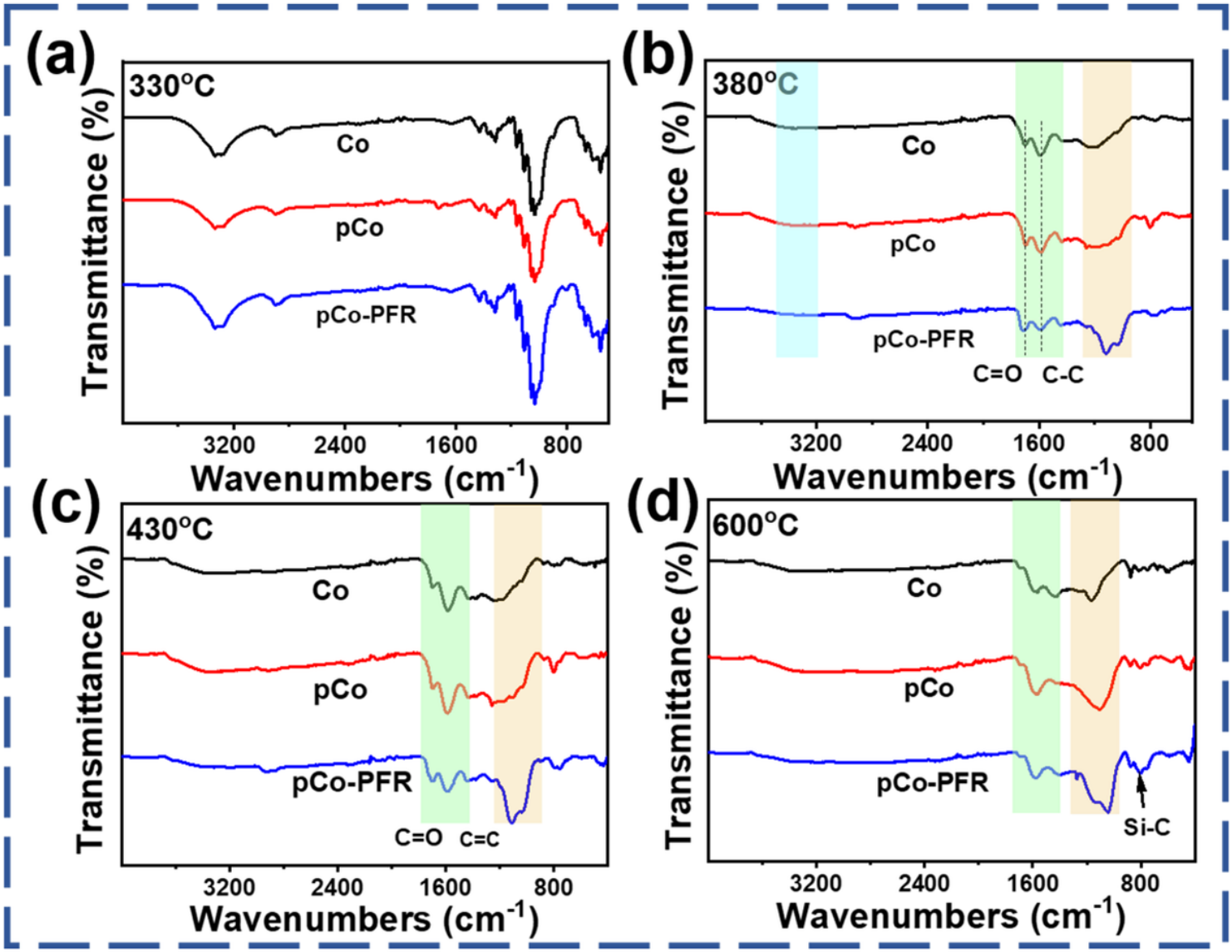

Figure 7

FT-IR spectra of Co, pCo and pCo-PFR after TGA in nitrogen at degradation temperature.

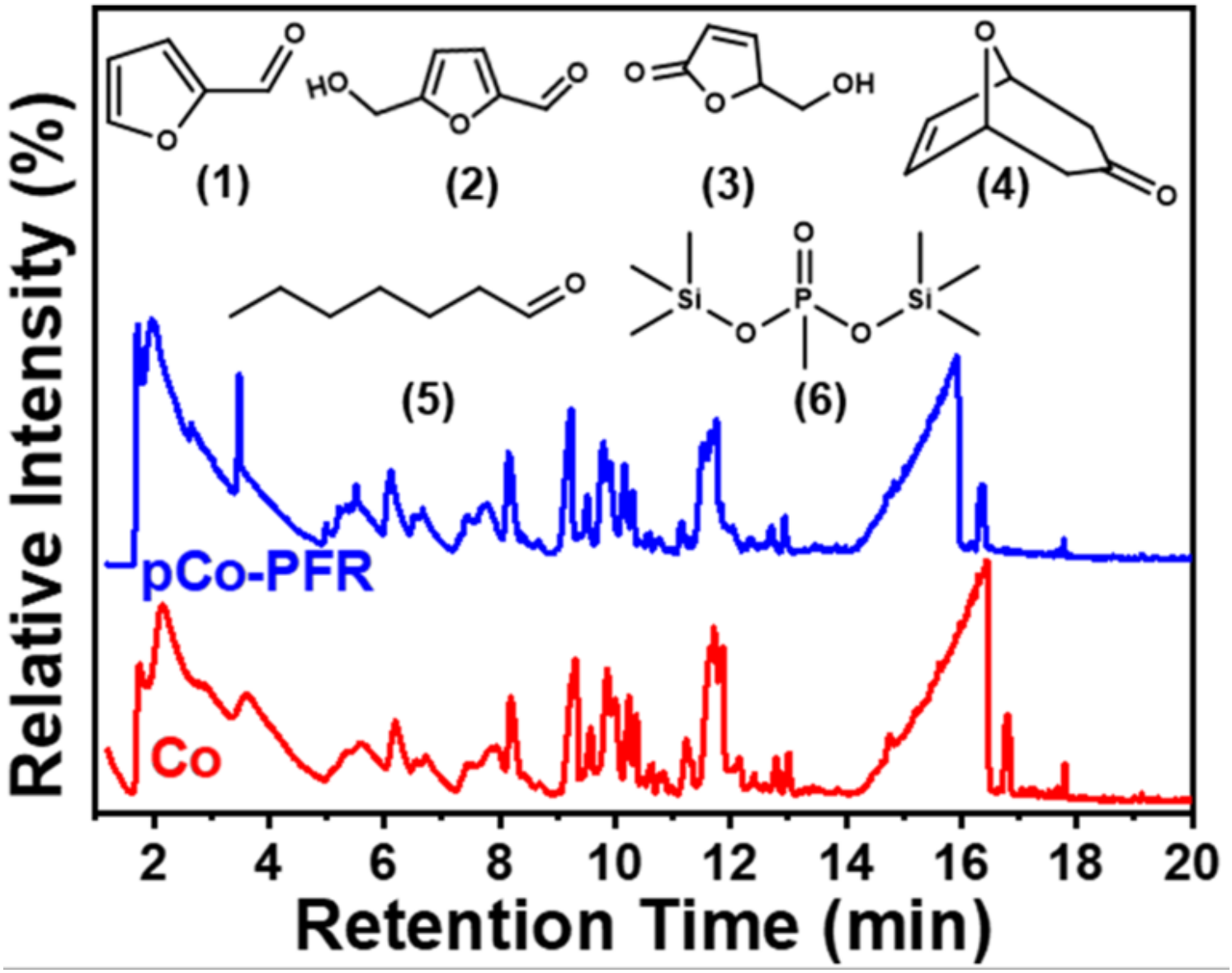

Figure 8

Pyrolysis gas chromatography mass spectrometry of Co and pCo-PFR at 380 oC.

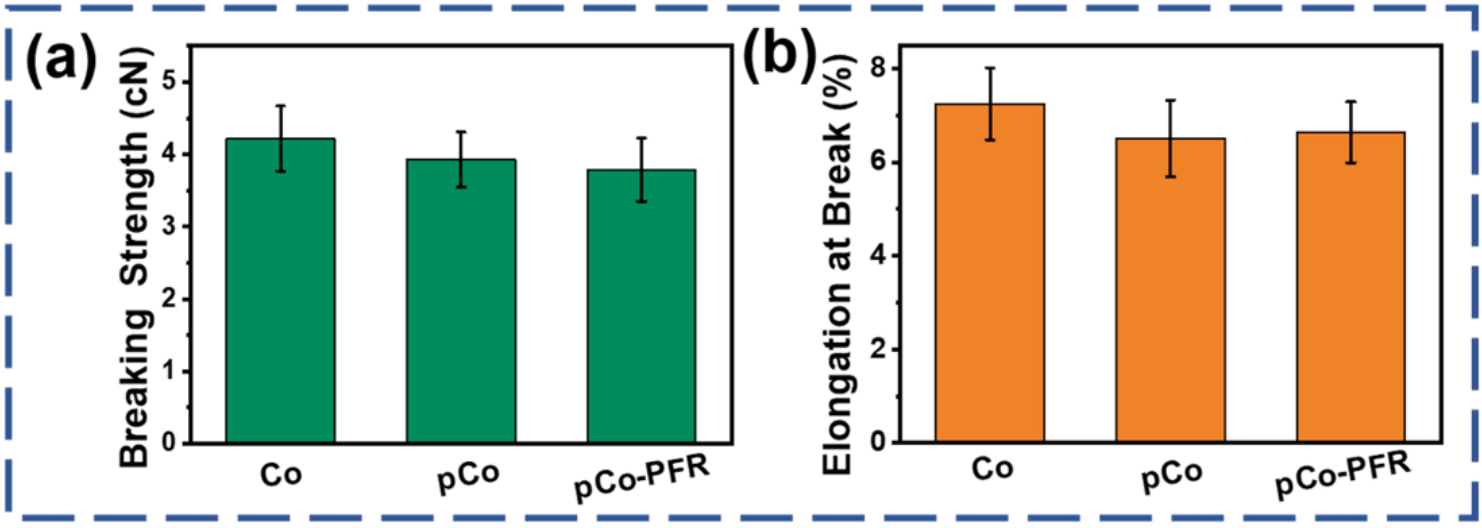

Figure 9

(a) Breaking strength and (b) elongation at break of Co, pCo and pCo-PFR.

Supplementary Files

This is a list of supplementary files associated with this preprint. Click to download.

- Graphicabstract.png
- scheme1.png